Development of the Cylindrical Wire Electrical Discharge Machining Process

Jun Qu and Albert J. Shih, Department of Mechanical and Aerospace Engineering, North Carolina State University
Ron O. Scattergood, Department of Materials Science and Engineering, North Carolina State University
Samuel B. McSpadden, High Temperature Materials Lab, Oak Ridge National Laboratory

Abstract

Results of applying the wire Electrical Discharge Machining (EDM) process to generate precise cylindrical forms on hard, difficult-to-machine materials are presented. A precise, flexible, and corrosion-resistant underwater rotary spindle was designed and added to a conventional two-axis wire EDM machine to enable the generation of free-form cylindrical geometries. A detailed spindle error analysis identifies the major source of error at different frequency. The mathematical model for the material removal of cylindrical wire EDM process is derived. Experiments were conducted to explore the maximum material removal rate for cylindrical and 2D wire EDM of carbide and brass work-materials. Compared to the 2D wire EDM, higher maximum material removal rates may be achieved in the cylindrical wire EDM. This study also investigates the surface integrity and roundness of parts created by the cylindrical wire EDM process. For carbide parts, an arithmetic average surface roughness and roundness as low as 0.68 and 1.7 μm, respectively, can be achieved. Surfaces of the cylindrical EDM parts were examined using Scanning Electron Microscopy (SEM) to identify the craters, sub-surface recast layers and heat-affected zones under various process parameters. This study has demonstrated that the cylindrical wire EDM process parameters can be adjusted to achieve either high material removal rate or good surface integrity.

1. Introduction

Electrical Discharge Machining (EDM) is a thermoelectric process that erodes workpiece material by a series of discrete electrical sparks between the workpiece and an electrode flushed by or immersed in a dielectric fluid. Unlike traditional cutting and grinding processes, which rely on the force generated by a harder tool or abrasive material to remove the softer work-material, the EDM process utilizes electrical sparks or thermal energy to erode the unwanted material and generate the desired shape. The EDM process particularly suitable for machining hard, difficult-to-machine materials. The EDM process has the ability to machine precise, complex, and irregular shapes with a CNC control system. In addition, the cutting force in the EDM process is small, which makes it ideal for fabricating parts with miniature features.

The concept of cylindrical wire EDM is illustrated in Fig. 1. A rotary axis is added to a conventional two-axis wire EDM machine to enable the generation of a cylindrical form. An example of the diesel fuel system injector plunger machined using the cylindrical wire EDM method is shown in Fig. 2.

The idea of using wire EDM to machine cylindrical parts has been reported by Dr. Masuzawa's research group at University of Tokyo [1-4]. These research activities were aimed to manufacture small-diameter pins and shafts. A wire guide was used to reduce the wire deflection during EDM of small-diameter shafts. Cylindrical pins as small as 5 μm in diameter can be machined [4]. The small-diameter pins can be used as tools for 3D micro-EDM applications [5, 6].

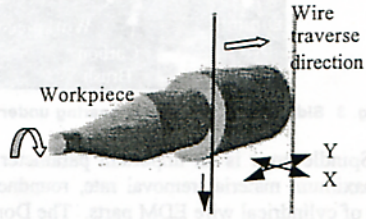

Fig. 1 The concept of cylindrical wire EDM process

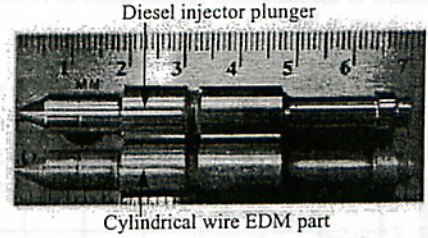

Fig. 2 A cylindrical wire EDM part with the same shape as the diesel engine injector plunger

In this study, instead of machining small-diameter pins, the focus is on exploring high material removal rate (MRR) in the cylindrical wire EDM process. The material removal rate data were not reported in Masuzawa's research [1-4]. In this study, two configurations to find the maximum material removal rate for cylindrical wire EDM were explored.

Investigations have been carried out to analyze and improve the surface integrity of parts created by die-sinking EDM [7, 8] and wire EDM [9, 10]. This study investigates the surface finish and roundness of cylindrical wire EDM parts and explores possible ways to adjust process parameters to achieve the best possible surface integrity.

Scanning Electron Microscopy (SEM) has been a common tool to examine EDM surfaces [8, 9]. This study uses SEM to examine the crater, recast layer and heat-affected zone to quantify and compare sub-surface damage for various EDM process parameters and MRR.

The spindle design and spindle error analysis methods are first presented in Sec. 2. The mathematical model for the material removal rate of cylindrical wire EDM is then derived in Sec. 3. The experimental results of the maximum MRR in the cylindrical wire EDM process are analyzed and compared to that of 2D wire EDM in Sec. 4. Results of surface roughness and roundness are presented in Sec. 5. SEM micrographs of the surfaces and cross-sections of the sub-surfaces of cylindrical wire EDM carbide parts are illustrated and discussed in Sec. 6.

2. Spindle Design and Error Analysis

The rotating workpiece is driven by a spindle, which is submerged in a tank of deionized water. This spindle must meet the following design criteria: Accuracy, Flexibility, High Current Electrical Connection, and Corrosion Resistance. The underwater spindle used in this study is shown in Fig. 3.

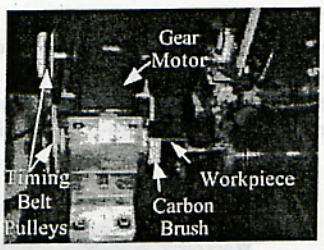

Fig. 3 Side view of the hybrid bearing underwater spindle

Spindle error is an important parameter that can affect the maximum material removal rate, roundness, and surface finish of cylindrical wire EDM parts. The Donaldson reversal principle [11] was applied to measure the spindle error. Results of the maximum spindle errors at 10 different speeds are shown in Fig. 4.

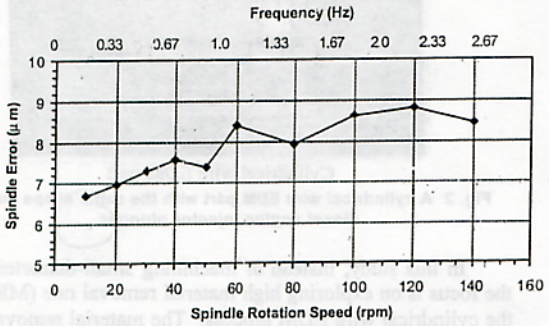

Fig. 4 Spindle error vs. rotational speed

Fourier transformation was applied to analyze the spindle runout data to identify the source of error, as shown in Fig. 5. Four major peaks can be identified.

(i) f_0: This is the major peak, which is caused by the off center error. The position of this peak always corresponds to the spindle rotational speed.

(ii) f_1: This is always equal to five times of f_0, possibly caused by the form error on bearing races.

(iii) f_3 and f_4: These two frequencies, 60 and 120 Hz, remain unchanged for different motor rotational speeds. They are possibly caused by the DC motor.

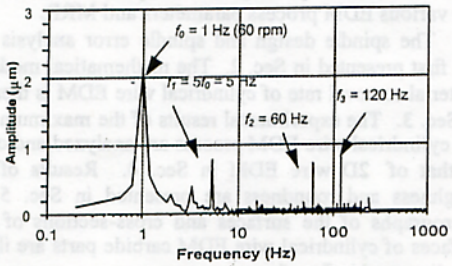

Fig. 5 Spindle rotation speed of 60 rpm

3. Material Removal Rate Modeling

The process parameters for modeling the material removal rate in cylindrical wire EDM of a free-form shape are illustrated in Fig. 6. R is the original radius of the workpiece. r_e is the radius of the effective circle, C_e, which equals the wire radius, r_w, plus the width of the gap between the wire and the workpiece. r is the distance from the lowest point of the effective circle to the rotational axis of the workpiece. v_f is the wire feed rate. α is the angle from the positive X-axis to v_f. The range of α is from $-\pi/2$ to $\pi/2$.

The Material Removal Rate (MRR) in cylindrical wire EDM of a free-form surface is derived in [12].

$$MRR = v_f \cdot \pi[(R^2 - r^2)\cos\alpha + 2rr_e(1 - \sin\alpha - \cos\alpha) + r_e^2(2 - 2\cos\alpha + (\frac{\pi}{2} - 2 - \alpha)\sin\alpha)] \quad (1)$$

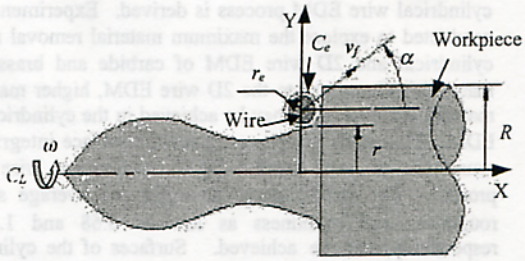

Fig. 6 Parameters in the cylindrical wire EDM process.

4. Experiment on the Maximum Material Removal Rate

The machine setup and process parameters for the cylindrical wire EDM experiment are listed in Table 1. Two parameters, the part rotational speed, ω, and wire feed rate, v_f, are varied in this study to investigate their effect on the cylindrical wire EDM of two different work-materials.

Table 1. Machine setup for the cylindrical wire EDM experiment.

Wire EDM machine	Brother HS-5100	
Wire manufacturer	Charmilles Tech., BercoCut	
Wire material	Brass	
Wire diameter (mm)	0.25	
Workpiece material	Brass	Carbide
Spark cycle (μs)	20	28
On-time (μs)	14	14
(Percentage of on-time)	(70%)	(50%)
Wire speed (mm/s)	15	18
Wire tension (g)	1500	1500
Gap voltage (V)	45	35

The maximum material removal rate (MRR_{max}) is an important indicator of the efficiency and cost-effective of the process. Tests are designed to find the MRR_{max} in both the cylindrical and 2D wire EDM. Two test configurations to measure the MRR_{max} in cylindrical wire EDM are illustrated in Fig. 7(a) and 7(b). Two 2D wire EDM tests, as shown in Figs. 7(c) and 7(d), were also conducted on the same work-material to evaluate the difference in MRR_{max}.

In Fig. 7(a), α is set to 0 degree and v_f is gradually increased to the limiting speed, when the short circuit error occurs. This v_f is recorded as $v_{f,max}$ and the MRR_{max} can be

calculated using Eq. (1). Another test configuration to measure MRR_{max} in cylindrical wire EDM, as shown in Fig. 7(b), has constant α and v_f. As the wire cuts into the workpiece, the material removal rate is gradually increased. At the position when the short circuit error occurs, the material removal rate is recorded as MRR_{max}. Two test configurations to find MRR_{max} for 2D wire EDM at different thickness are shown in Figs. 7(c) and 7(d). The v_f was gradually increased to find the MRR_{max}. Results of MRR_{max} are summarized in Tables 2 to 4.

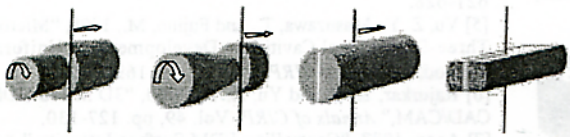

(a) Cylindrical test I (b) Cylindrical test II (c) 2D test I (d) 2D test II

Fig. 7 Four test configurations to find the maximum MRR

Table 2. MRR_{max} for the cylindrical wire EDM test with α = 0 and gradually increasing v_f.

Material	R (mm)	3.18			2.54	
	r (mm)	2.54	1.59	0.75	1.59	0.75
Brass	$v_{f,max}$ (mm/min)	5.72	2.69	2.13	5.33	3.46
	MRR_{max} (mm³/min)	65.2	64.1	63.7	65.7	64.0
Carbide	$v_{f,max}$ (mm/min)	1.42	0.81	0.66	1.55	1.02
	MRR_{max} (mm³/min)	16.2	19.3	19.7	19.1	18.9

Table 3. MRR_{max} for the cylindrical wire EDM test with constant α and v_f.

Material	v_f (mm/min)	α (degree)	-15	-30	-45
Brass	3.81	r_{min} (mm)	2.16	2.01	1.65
		MRR_{max} (mm³/min)	65.5	68.3	69.6
Carbide	1.02	r_{min} (mm)	2.02	1.95	1.17
		MRR_{max} (mm³/min)	19.1	18.7	20.9

Table 4. MRR_{max} for the 2D wire EDM test.

Material	t (mm)	r_e (mm)	$v_{f,max}$ (mm/min)	MRR_{max} (mm³/min)
Brass	6.35	0.183	23.9	55.5
	3.23	0.183	37.8	44.7
Carbide	6.35	0.163	4.32	8.94
	3.23	0.163	8.00	8.42

Several observations can be extracted from the results.

1. The brass has much higher MRR_{max} than the carbide.
2. The results from the two test configurations for cylindrical wire EDM at different sizes and angles are close to each other. This verifies the concept as well as the mathematical model for the cylindrical wire EDM material removal rate.
3. The MRR_{max} for cylindrical wire EDM in Tables 2 and 3 is greater than the 2D wire EDM results in Table 4. The possible cause may be better flushing conditions in the cylindrical wire EDM. In 2D wire EDM, as shown in Fig. 9(c), a narrow gap exists and affects the flow of high pressure water jets. Such situation does not exist in the cylindrical wire EDM.
4. The MRR_{max} for 2D wire EDM changes slightly with thickness.

5. Surface Finish and Roundness

Cylindrical wire EDM experiments were conducted to investigate the surface finish and roundness generated under different process parameters and to verify the surface finish model [13]. The goal of the experiment was to achieve the best possible surface finish and roundness by adjusting two critical process parameters, the wire feed rate and pulse on-time. The cutting configuration shown in Fig. 7(a) with α = 0, R = 2.59 mm, and r = 2.54 mm was used.

Figure 8 shows the surface finish and roundness results. The shorter pulse on-time and lower feed rate, in general, created better surface finish and roundness. Shorter pulse on-time generates smaller sparks, which, in turn, creates smaller craters and better surface finish. This can be verified in the SEM micrographs of EDM surfaces. The best R_a and roundness generated on carbide are 0.68 and 1.7 μm, respectively. These values are comparable to that of rough grinding, which makes the cylindrical wire EDM process suitable for precision machining of the difficult-to-machine materials.

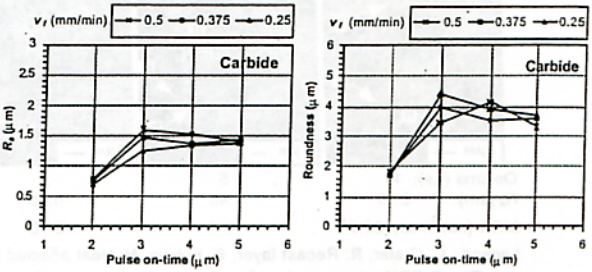

Fig. 8 The surface finish and roundness of cylindrical WEDM parts.

6. SEM Micrographs of EDM Surface and Sub-Surface

SEM is used to examine the surface and sub-surface of cylindrical wire EDM carbide parts.

6.1 Craters. The cylindrical wire EDM surfaces are observed using the SEM machine to compare the surface texture and crater size. Under shorter pulse on-time, electrical sparks generate smaller craters on the surface. For carbide parts, as shown in Fig. 9, the rough estimate of the crater size is about 50, 30, and 20 μm under 14, 5, and 2 μs pulse on-time, respectively.

6.2 Sub-Surface Recast Layers and Heat-Affected Zones. The recast layer is defined as the material melted by electrical sparks and resolidified on the surface without being ejected nor removed by flushing. Below the recast layer is the heat-affected zone. For the carbide material, the cobalt matrix melts and resolidifies in the heat-affected zone. The molten cobalt fills the pores in the tungsten carbide. This is observed in the SEM micrographs of the carbide cross-section and is used to identify the depth of heat-affected zone. Rajurkar and Pandit [14] have studied the recast layer and heat-affected zones of EDM surfaces and developed a thermal model to predict the thicknesses of damaged layers. Anon [7] has studied the sub-surface heat-affected zones and recast layers of steel and tungsten carbide using the die-sinking EDM and have summarized and explained the possible causes for EDM surface defects.

SEM micrographs of the cross-section of carbide parts are shown in Fig. 9. The recast layer, bubbles in the recast

layer, and heat affected zone of three carbide samples are identified. Under high MRR at 14 μs pulse on-time, the recast layer, about 3 μm thick, can be clearly recognized on the surface. Thinner recast layers, less than 2 μm, exist on samples machined using shorter pulse on-time. Bubbles can be identified in the recast layers of all three carbide samples. Anon [7] has proposed that these micro-bubbles were generated by thermal stresses and tension cracking in the recast layer. As shown in Fig. 9, the depth of the heat-affected zone is estimated to be about 4, 3, and 2 μm on the three carbide samples with 14, 5, and 2 μs pulse on-time, respectively.

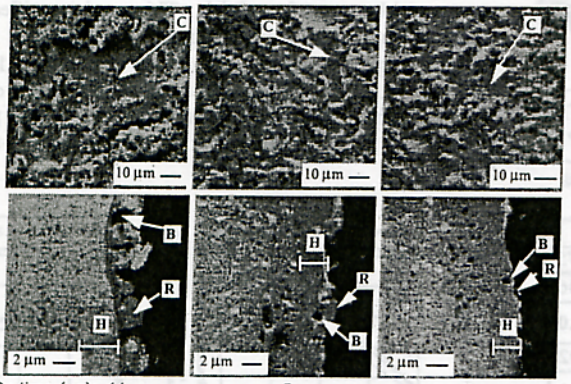

On-time (μs):	14	5	2
R_a (μm):	2.53	1.40	0.68
MRR (mm^3/min):	29.0	17.1	5.70

Legend : C: Crater, R: Recast layer, B: Bubble, H: Heat affected zone.

Fig. 9 SEM micrographs of surfaces and cross-sections.

4. Conclusion

The feasibility of applying the cylindrical wire EDM process for high material removal rate machining of free-form cylindrical geometries was demonstrated in this study. The mathematical model for the material removal rate of cylindrical wire EDM of free-form surfaces was derived. Two experimental configurations designed to find the maximum material removal rates in cylindrical wire EDM were proposed. Results of each test configurations match each other, which validates the concept. The maximum material removal rate for the cylindrical wire EDM was higher than that in 2D wire EDM of the same work-material. This indicates that the cylindrical wire EDM is an efficient material removal process. The surface integrity and roundness of cylindrical wire EDM carbide and brass parts were investigated. Experiments demonstrated that good surface finish and roundness could be achieved in the cylindrical wire EDM process. The craters, recast layers, and heat-affected zones were observed, and their sizes were estimated using the SEM.

Acknowledgement

The authors gratefully acknowledge the support by National Science Foundation Grant #9983582 (Dr. K. P. Rajurkar, Program Director). Portion of this research was sponsored by the User program in the High Temperature Material Lab, Oak Ridge National Lab and the Heavy Vehicle Propulsion Systems Materials Program, Office of Transportation Technologies, US Department of Energy.

References

[1] Masuzawa, T., Fujino, M., Kobayashi, K., and Suzuki, T., 1985, "Study on Micro-Hole Drilling by EDM," *Bull. Japan Soc. of Prec. Eng.*, Vol. 20, No. 2, pp. 117-120.

[2] Kuo, C.-L., Masuzawa, T., and Fujino, M., 1992, "High-Precision Micronozzle Fabrication," *IEEE Micro Electro Mechanical Systems '92, Travemunde Germany*, Feb. 4-7, pp.116-121.

[3] Masuzawa, T., Kuo, C.-L., and Fujino, M., 1994, "A Combined Electrical Machining Process for Micronozzle Fabrication," *Annals of CIRP*, Vol. 43, pp.189-192.

[4] Masuzawa, T. and Tonshoff, H. K., 1997, "Three-Dimensional Micromachining by Machine Tools," *Annals of CIRP*, Vol. 46, pp. 621-628.

[5] Yu, Z. Y., Masuzawa, T., and Fujino, M., 1998, "Micro-EDM for Three-Dimensional Cavities - Development of Uniform Wear Method," *Annals of CIRP*, Vol. 47, pp. 169-172.

[6] Rajurkar, K. P. and Yu, Z. Y., 2000, "3D Micro-EDM Using CAD/CAM," *Annals of CIRP*, Vol. 49, pp. 127-130.

[7] Anon, 1987, "Controlling EDM Surface Integrity," American Machinist & Automated Manufacturing, Vol. 131, No. 11, pp. 80-83.

[8] Rajurkar, K. P. and Royo, G. F., 1989, "Effect of R.F. Control and Orbital Motion on Surface Integrity of EDM Components," *Journal of Mechanical Working Technology*, Vol. 20, pp. 341-352.

[9] Williams, R. E. and Rajurkar, K. P., 1991, "Study of Wire Electrical Discharge Machined Surface Characteristics," *Journal of Mechanical Processing Technology*, Vol. 28, pp. 127-138.

[10] Gokler, M. I. and Ozanozgu, A. M., 2000, "Experimental Investigation of Effects of Cutting Parameters on Surface Roughness in the WEDM Process," *International Journal of machine Tools & Manufacture*, Vol. 40, pp. 1831-1848.

[11] Slocum, A. H., 1992, *Precision Machine Design*, Prentice Hall.

[12] Qu, J., Shih, A. J., and Scattergood, R., "Development of the Cylindrical Wire Electrical Discharge Machining Process, Part I: Concept, Design, and Material Removal Rate," Submitted to *Journal of Manufacturing Science and Engineering.*

[13] Qu, J., Shih, A. J., and Scattergood, R., "Development of the Cylindrical Wire Electrical Discharge Machining Process, Part II: Surface Integrity and Roundness," Submitted to *Journal of Manufacturing Science and Engineering.*

[14] Rajurkar, K. P. and Pandit, S. M., 1984, "Quantitative Expressions for Some Aspects of Surface Integrity of Electro-Discharge Machined Components," *Transactions of ASME Journal of Engineering for Industry,* Vol. 106, No. 2, pp. 171-177.